# Turbulence Energy and Diffusion Transport of Third-Moments in a Separating and Reattaching Flow

R. S. Amano,* P. Goel,† and J. C. Chai‡
*University of Wisconsin, Milwaukee, Wisconsin*

**For accurate prediction of turbulent flow in separated and reattaching regions, it is necessary to incorporate second- and third-moments of turbulent fluctuations. The turbulence energy and the energy dissipation rate equations are modified by incorporating second-order closure. Moreover, a transport equation model for the third-order closure with a near-wall correction is developed for the evaluation of the diffusive action of the second-moments. After comparison of the results with experimental data, it is concluded that the models developed here improve the prediction of triple-velocity correlations in both recirculating and redeveloping flow regions.**

## Nomenclature

| | |
|---|---|
| $a_{ij}$ | = anisotropy |
| $C_D, C_k, C_\ell, C_\gamma,$ $C_{\gamma W}, C_\epsilon, C_{\epsilon 1}, C_{\epsilon 2}$ | = constants used in turbulence model |
| $C_f$ | = skin friction coefficient, $\tau_w/(1/2\rho U_{IN}^2)$ |
| $C_{ij}$ | = coefficients for near-wall Reynolds stresses |
| $C_p$ | = pressure coefficient, $(P - P_{\text{ref}})/(1/2\rho U_{IN}^2)$ |
| $f_w$ | = function for wall correction |
| $G$ | = generation rate of turbulence kinetic energy $k$ |
| $G_{ij}$ | = generation rate of Reynolds stresses |
| $H$ | = step height |
| $H_{ij}$ | = secondary generation rate of Reynolds stresses |
| $k$ | = turbulence kinetic energy, $\overline{u_i^2}$ |
| $p$ | = pressure fluctuation |
| $P$ | = mean pressure |
| $u$ | = fluctuating velocity in $x$ direction |
| $U$ | = mean velocity |
| $U_{IN}$ | = inlet stream velocity |
| $v$ | = fluctuating velocity in $y$ direction |
| $w$ | = fluctuating velocity in $z$ direction |
| $x, y, z$ | = Cartesian coordinates |
| $x_R$ | = location of flow reattachment measured from the step |
| $y^+$ | = dimensionless distance from wall to the first numerical node point, $(\tau_w/\rho)^{1/2} y/\nu$ |
| $\alpha_1, \alpha_2, \alpha_3, \alpha_4$ | = constants used in Eq. (18) |
| $\delta_{ij}$ | = Kronecker delta |
| $\epsilon$ | = energy dissipation rate |
| $\nu$ | = kinematic viscosity |
| $\rho$ | = density |
| $\tau_w$ | = wall shear stress |

*Subscripts*

| | |
|---|---|
| $i, j, k, \ell, m$ | = tensor notations |
| ref | = reference station ($x/H = -4$) conditions |

## Introduction

IN computations of the flow in a gas turbine combustor, it is necessary to evaluate turbulence quantities in order to accurately predict the heat transfer and chemical reaction rates. However, the complexity of the flow structure created by flow separation and reattachment would make the analysis rather difficult. For this reason, a basic study of the reattaching shear layer is needed in order to develop a universal turbulence model that predicts flow behaviors without many limitations.

A large number of experimental studies on this subject have been reported in the last two decades (Eaton and Johnston,[1] for example). Despite the number of studies on separated and reattaching shear flows, higher-order turbulence models that are capable of accurately predicting these reattaching and recirculating flows have not yet been developed. This is partly because it is hard to obtain accurate measurements near the reattaching point due to its intrinsically unsteady nature and partly because the experimental technique has limitations.

The Reynolds stresses in the reattachment zone were obtained by Etheridge and Kemp,[2] Kim et al.,[3] Smyth,[4] and others in backward-facing step flows. It has been shown that the turbulence energy level reaches a peak value approximately one step height upstream of the reattachment point along the shear layer and then decays rapidly in the streamwise direction toward the wall, although it decays relatively slowly along the wall in the wall vicinity region. This feature is in contrast with free shear flows, which do not have the constraint of the solid wall. It is also noted that the recirculating zone affects the reattaching shear layer, resulting in higher turbulence energy levels near the reattachment zone.

Measurements of higher-order turbulence quantities near the reattachment zone have been made by Chandrsuda and Bradshaw[5] and Driver and Seegmiller.[6] The triple-velocity products were measured by Chandrsuda and Bradshaw by using a hot-wire anemometer for a channel with a width of 3.5 step heights. Driver and Seegmiller used a channel with a width of 9 step heights. In their case, the boundary-layer thickness at the step was about 1.5 step heights, with an inviscid core region outside the separating layer. They measured the second- and third-moments of turbulence velocity fluctuations with an LDV.

The third-moment closures have been studied in detail by several researchers.[7-10] The models obtained by them are all in algebraic equations. The models of Daly and Harlow[7] and Shir[8] correlate the triple-velocity products with the products of the Reynolds stresses and their gradients. Hanjalic and Launder[9] obtained an algebraic equation for the triple-velocity product from the triple-velocity transport equation by neglecting the convection, diffusion, generation due to mean strains, and dissipation rates. Unlike the previously mentioned models, Cormack et al.[10] obtained an expression for the triple-velocity products simply by correlating the symmetric form of anisotropy of turbulence by comparing it with a

Received March 4, 1986; revision received May 6, 1987. 

*Associate Professor, Department of Mechanical Engineering.
†Graduate Student, Department of Mechanical Engineering.
‡Research Assistant, Department of Mechanical Engineering.

consensus of experimental data available for freejets, wall flows, and wakes.

This paper deals with a theoretical study of the separating and reattaching flow downstream of a step. The second-moment approach of the velocity fluctuation is applied to the transport equations of turbulence energy and the energy dissipation rate. Upon comparison of the computed results with available experimental data, optimum coefficients for the diffusion rates are obtained. Moreover, behavior of all the terms in the $k$ equation computed with the present model is also compared with the conventional Boussinesq treatment.

All of the algebraic models for third-moment closures seem to be reasonable for computations of parabolic flows. However, it has been shown by the present authors[11] that the predictions of such third-moments with algebraic models are far from reliable experimental data for predicting reattaching shear flows; the disagreement is remarkable, particularly near the reattaching region. For this reason, this study is further extended to the development of transport equations for third-moments with the incorporation of a near-wall correction factor. The triple-velocity products across the reattaching shear layer are investigated by making comparisons with the existing third-moment algebraic models.

## Turbulence Models

### Second-Moment Closures

The transport equations which describe the Reynolds-stress variation in the flowfield are derived as

$$U_\ell \frac{\partial \overline{u_i u_j}}{\partial x_\ell} = -\underbrace{\left(\overline{u_j u_\ell}\frac{\partial U_i}{\partial x_\ell} + \overline{u_i u_\ell}\frac{\partial U_j}{\partial x_\ell}\right)}_{\text{(i)}} + \underbrace{\overline{\frac{p}{\rho}\left(\frac{\partial u_i}{\partial x_j} + \frac{\partial u_j}{\partial x_i}\right)}}_{\text{(ii)}}$$

$$+ \frac{\partial}{\partial x_\ell}\left[\nu\frac{\partial \overline{u_i u_j}}{\partial x_\ell} - \underbrace{\overline{\frac{p}{\rho}\left(\delta_{j\ell}u_i + \delta_{i\ell}u_j\right)} - \overline{u_i u_j u_\ell}}_{\text{(iii)}}\right] - \underbrace{2\nu\overline{\frac{\partial u_i}{\partial x_\ell}\frac{\partial u_j}{\partial x_\ell}}}_{\text{(iv)}} \tag{1}$$

from which the turbulence kinetic energy equation is also derived. The definition of the turbulence kinetic energy is

$$k \equiv \overline{u_i u_i}/2 \tag{2}$$

There are two ways to obtain $k$: one is to solve Eq. (1) for $\overline{u^2}$, $\overline{v^2}$, and $\overline{w^2}$ and substitute the results into Eq. (2), and the other way is to formulate the transport equation for $k$ itself. When the problem is in a two-dimensional Cartesian coordinate system, the number of equations which need to be solved is the same using either technique. In this paper, the transport equation for $k$ is examined in the second-moment closure rather than solving all three normal components of the Reynolds stresses. This is because the $k$ equation is widely used as an indicator of turbulence levels. Thus, the $k$ equation cannot be omitted when one is solving the two-equation model or the algebraic-stress model.

Upon contracting Eq. (1) by setting $j$ equal to $i$ and dividing by two, the $k$ equation yields as

$$U_\ell \frac{\partial k}{\partial x_\ell} = \underbrace{-\overline{u_i u_\ell}\frac{\partial U_i}{\partial x_\ell}}_{\text{(i)}} + \frac{\partial}{\partial x_\ell}\left(\underbrace{\nu\frac{\partial k}{\partial x_\ell}}_{\text{(ii)}} - \underbrace{\overline{\frac{p}{\rho}u_\ell}}_{\text{(iii)}} - \underbrace{\overline{\frac{u_i u_i u_\ell}{2}}}_{\text{(iv)}}\right)$$

$$\underbrace{-\nu\overline{\frac{\partial u_i}{\partial x_\ell}\frac{\partial u_i}{\partial x_\ell}}}_{\text{(v)}} \tag{3}$$

Term (i) represents the generation rate, and terms (ii)–(iv) correspond to the diffusion rate. Term (v) represents the dissipation of the turbulence energy which is determined by solving the $\epsilon$ equation. Here, terms (iii) and (iv) may be replaced by the following form:

$$\text{(iii)} + \text{(iv)} = \frac{\partial}{\partial x_\ell}\left(C_k \frac{k}{\epsilon}\overline{u_i u_\ell}\frac{\partial k}{\partial x_i}\right) \tag{4}$$

In the computation, the viscous term (ii) is retained in order to account for near-wall effects.

To solve for the Reynolds stresses, Eq. (1) was closed as follows:

$$U_\ell \overline{\frac{\partial u_i u_j}{\partial x_\ell}} = -\left(\overline{u_j u_\ell}\frac{\partial U_i}{\partial x_\ell} + \overline{u_i u_\ell}\frac{\partial U_j}{\partial x_\ell}\right) + \phi_{ij} + D_{ij} - \frac{2}{3}\delta_{ij}\epsilon \tag{5}$$

where the pressure-strain correlation $\phi_{ij}$ is divided into two parts: the Rotta term[12] and the rapid term.[13] The diffusion rate $D_{ij}$ is conventionally approximated as

$$D_{ij} = \frac{\partial}{\partial x_\ell}\left(C_D \frac{k}{\epsilon}\overline{u_\ell u_m}\frac{\partial \overline{u_i u_j}}{\partial x_m}\right) \tag{6}$$

for the computation of $\overline{u_i u_j}$. A more extensive model for the triple-velocity products $\overline{u_i u_j u_k}$ is given in the next subsection. The energy dissipation rate equation is given as

$$U_\ell \frac{\partial \epsilon}{\partial x_\ell} = -\frac{\epsilon}{k}\left(\underbrace{C_{\epsilon 1}\overline{u_i u_\ell}\frac{\partial U_i}{\partial x_\ell}}_{\text{(i)}} + \underbrace{C_{\epsilon 2}\nu\overline{\frac{\partial u_i}{\partial x_\ell}\frac{\partial u_i}{\partial x_\ell}}}_{\text{(ii)}}\right)$$

$$- \frac{\partial}{\partial x_\ell}\left(\underbrace{\nu u_\ell \overline{\frac{\partial u_i}{\partial x_\ell}\frac{\partial u_i}{\partial x_\ell}}}_{\text{(iii)}} + \underbrace{2\frac{\partial \nu}{\partial \rho}\overline{\frac{\partial p}{\partial x_j}\frac{\partial u_\ell}{\partial x_j}}}_{\text{(iv)}} - \underbrace{\nu\frac{\partial \epsilon}{\partial x_\ell}}_{\text{(v)}}\right) \tag{7}$$

where $C_{\epsilon 1} = 1.45$ and $C_{\epsilon 2} = 1.92$, which are the values currently used by a number of researchers.

The generation (i) and destruction (ii) terms are evaluated using a direct approach. The diffusion rate is modified in a form similar to that of Eq. (4):

$$\text{(iii)} + \text{(iv)} = \frac{\partial}{\partial x_\ell}\left(C_\epsilon \frac{k}{\epsilon}\overline{u_i u_\ell}\frac{\partial \epsilon}{\partial x_i}\right) \tag{8}$$

Note that term (v) is also used to account for viscous effects as before. The coefficients $C_k$ and $C_\epsilon$ were recommended to be 0.31 and 0.15, respectively, by Pope and Whitelaw.[14] More extensive tests for these coefficients are made for the computation of reattaching shear flows, and better coefficients are recommended in the discussion section.

### Third-Moment Closures

It is known that the higher moments of the turbulence fluctuating velocity vary rapidly in the shear layer reattaching to a solid wall.[5] This affects the accuracy of the computation in the diffusion term of the Reynolds stresses because it contains the third-moment velocity fluctuations. Again, it is evident that the triple-velocity products need to be evaluated in a transport equation model rather than in an algebraic form because the convection and generation of the triple-velocity products have to be taken suitably into account according to the change in mean strain rates.[11] For this reason, full trans-

port equation models of the triple-velocity products are developed for predictions in the reattaching shear flows.

The complete equations are given as

$$U_\ell \frac{\partial}{\partial x_\ell}\left(\overline{u_i u_j u_k}\right) = -\left(\overline{u_i u_j u_\ell}\frac{\partial U_k}{\partial x_\ell} + \overline{u_j u_k u_\ell}\frac{\partial U_i}{\partial x_\ell} + \overline{u_k u_i u_\ell}\frac{\partial U_j}{\partial x_\ell}\right)$$

(i)

$$+\left(\overline{u_i u_j}\,\overline{\frac{\partial u_k u_\ell}{\partial x_\ell}} + \overline{u_j u_k}\,\overline{\frac{\partial u_i u_\ell}{\partial x_\ell}} + \overline{u_k u_i}\,\overline{\frac{\partial u_j u_\ell}{\partial x_\ell}}\right)$$

(ii)

$$-\frac{\partial}{\partial x_\ell}\left(\overline{u_i u_j u_k u_\ell}\right) - \frac{1}{\rho}\left(\overline{u_i u_j \frac{\partial p}{\partial x_k}} + \overline{u_j u_k \frac{\partial p}{\partial x_i}} + \overline{u_k u_i \frac{\partial p}{\partial x_j}}\right)$$

(iii) (iv)

(9)

where terms (i) and (ii) represent the generations due to the mean strain rate and turbulence stresses, respectively. Terms (iii) and (iv) both represent the diffusion of the triple-velocity products. In Eq. (9), the terms associated with the molecular viscosity are neglected.

The quadruple correlation in term (iii) is decomposed into the products of the second-order moments from the normal law according to Hanjalic and Launder[9]:

$$\overline{u_i u_j u_k u_\ell} = \overline{u_i u_j}\cdot\overline{u_k u_\ell} + \overline{u_i u_k}\cdot\overline{u_j u_\ell} + \overline{u_i u_\ell}\cdot\overline{u_j u_k} \tag{10}$$

The stress-pressure correlation in term (iv) can be approximated as

$$\text{(iv)} = -\Gamma\overline{u_i u_j u_k} \tag{11}$$

where $\Gamma$ is an inverse function of the turbulence time scale.

The final form of Eq. (9) is given as

$$U_\ell \frac{\partial}{\partial x_\ell}\left(\overline{u_i u_j u_k}\right) = -\left(\overline{u_i u_j u_\ell}\frac{\partial U_k}{\partial x_\ell} + \overline{u_j u_k u_\ell}\frac{\partial U_i}{\partial x_\ell} + \overline{u_k u_i u_\ell}\frac{\partial U_j}{\partial x_\ell}\right)$$

$$-\left(\overline{u_k u_\ell}\,\overline{\frac{\partial u_i u_j}{\partial x_\ell}} + \overline{u_j u_\ell}\,\overline{\frac{\partial u_i u_k}{\partial x_\ell}} + \overline{u_i u_\ell}\,\overline{\frac{\partial u_j u_k}{\partial x_\ell}}\right) - \Gamma\overline{u_i u_j u_k} \tag{12}$$

In our original work,[15] the function $\Gamma$ was proposed as

$$\Gamma = C_\gamma \frac{\epsilon}{k} \tag{13}$$

where $C_\gamma$ is an empirical constant. The value of $C_\gamma$ has been recommended to be 5.8 for the best agreement with several experimental data for $\overline{u_i u_j u_k}$.[5,6] The model with Eq. (13) is referred to as a "high-Reynolds-number model," since this model does not have any terms which take the viscous wall effects into account. As a result, it was shown that the levels of the triple-velocity products predicted by using the high-Reynolds-number model were very high in the near-wall region.

In this paper, a low-Reynolds-number model for the triple-velocity correlation is proposed in order to account for the near-wall effects. According to turbulent boundary-layer theory, the turbulence energy dissipation rate $\epsilon$ is represented by $2\nu(\partial k^{1/2}/\partial y)^2$ in the viscous sublayer and by $k^{3/2}/(C_\ell y)$ in the fully turbulent core region of the boundary layer, where $C_\ell$ is an empirical constant whose value is 2.55. Due to the finer-scale eddies generated in the near-wall region, the turbulence dissipation rate increases appreciably toward the solid wall. In order to compensate for this effect, the function $\Gamma$ is formulated as

$$\Gamma = \frac{C_\gamma}{k}\left\{\epsilon + \max\left[C_{\gamma w}\frac{k^{3/2}}{C_\ell y}, 2\nu\left(\frac{\partial k^{1/2}}{\partial y}\right)^2\right]\right\} \tag{14}$$

The relative magnitudes of each term within the braces of Eq. (14) are compared in Fig. 1. The values for coefficients $C_\gamma$ and $C_{\gamma w}$ are found to be 2.0 and 8.0, respectively, for the best fit with a consensus of several experimental data.

The preceding model is compared with four existing models. These are given as follows:

1) The model of Daly and Harlow[7]:

$$\overline{u_i u_j u_k} = -0.25\frac{k}{\epsilon}\overline{u_k u_\ell}\,\overline{\frac{\partial u_i u_j}{\partial x_\ell}} \tag{15}$$

2) The model of Hanjalic and Launder[9]:

$$\overline{u_i u_j u_k} = -0.11\frac{k}{\epsilon}\left[\overline{u_\ell u_j}\,\overline{\frac{\partial u_i u_k}{\partial x_\ell}} + \overline{u_\ell u_i}\,\overline{\frac{\partial u_j u_k}{\partial x_\ell}} + \overline{u_\ell u_k}\,\overline{\frac{\partial u_i u_j}{\partial x_\ell}}\right] \tag{16}$$

3) The model of Shir[8]:

$$\overline{u_i u_j u_k} = -0.04\frac{k^2}{\epsilon}\overline{\frac{\partial u_i u_j}{\partial x_k}} \tag{17}$$

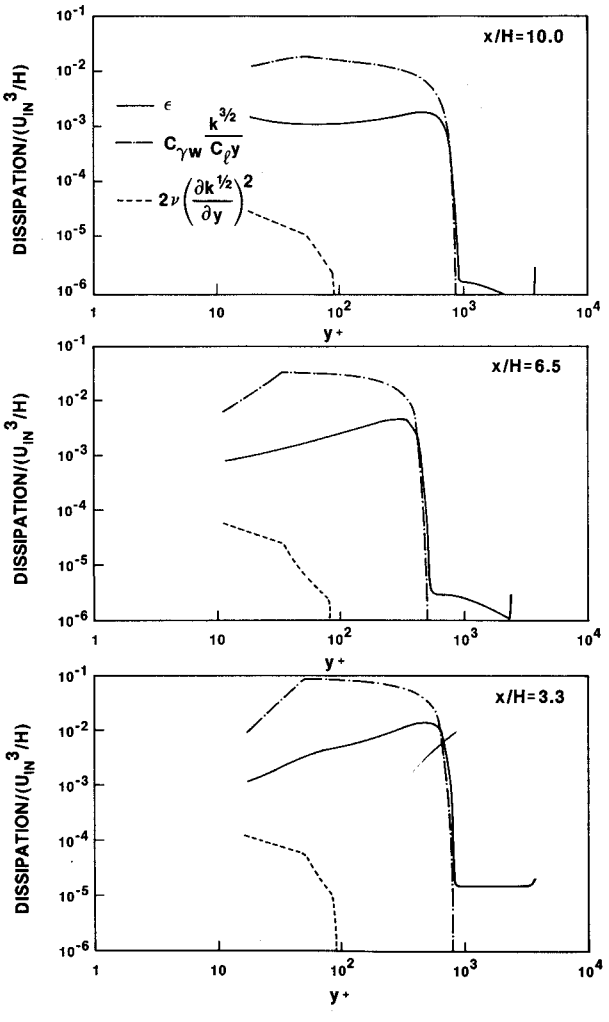


**Fig. 1 Turbulence dissipation rate in the near-wall region.**

4) The model of Cormack et al.[10]:

$$\overline{u_i u_j u_k} = 4\frac{k^2}{\epsilon}\left[2\alpha_1\left(\delta_{ij}\delta_{k\ell}+\delta_{ik}\delta_{j\ell}+\delta_{kj}\delta_{i\ell}\right)\frac{\partial k}{\partial x_\ell} + \alpha_2\left(a_{ik,j}+a_{ij,k}+a_{kj,i}\right)\right] + 2\frac{k}{\epsilon}\left[2\alpha_3\left(\delta_{ik}a_{j\ell}+\delta_{ij}a_{k\ell}+\delta_{jk}a_{i\ell}\right)\frac{\partial k}{\partial x_\ell} + \alpha_4\left(a_{ik}a_{j\ell,\ell}+a_{ij}a_{k\ell,\ell}+a_{jk}a_{i,\ell,\ell}\right)\right] \quad (18)$$

where

$$a_{ij} = \overline{u_i u_j} - \frac{2}{3}\delta_{ij}k \qquad a_{ij,k} = \frac{\partial a_{ij}}{\partial x_k} \quad (19)$$

The coefficients are given in Table 1.

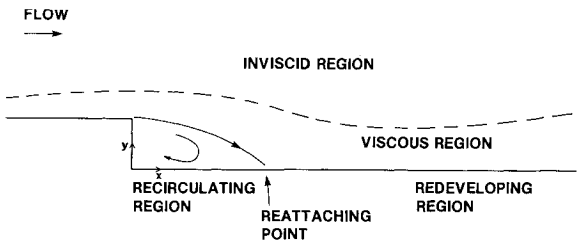


Fig. 2 Computational domain.

## Numerical Model

The transport equations described in the preceding section were solved by using the finite-volume method of Patankar.[16] At the inlet of the flowfield considered (Fig. 2), prescribed values are given to all variables; they are basically taken from the experimental data with which the results are compared. Along the top portion and the outflow section of the computational domain, the continuous boundary condition (zero gradient of properties in the stream direction) is applied.

At the wall boundaries, the "modified wall law" is used to specify mean velocities, turbulence kinetic energy, energy dissipation rate, and the Reynolds stresses. This model was developed by Amano[17] for the computation of separating and reattaching flows by incorporating the streamwise curvature effect. The near-wall values for $\overline{u_i u_j}$ are determined by using the correlation equation developed by Amano and Goel.[18] The values for the triple-velocity products at the wall-adjacent node points are evaluated by using Shir's algebraic formula [Eq. (17)].

The solution domain varies depending on whether the step flows of Chandrsuda and Bradshaw[5] or Driver and Seegmiller[6] are used. The domain of the former is $50 \times 3.5\ H$ with a solid wall at the upper boundary, whereas that of the latter

Table 1 Coefficients for $\alpha_i$

| $\alpha_1$ | $\alpha_2$ | $\alpha_3$ | $\alpha_4$ |
|---|---|---|---|
| $-8.14\times10^{-3}$ | $-1.72\times10^{-2}$ | $-4.80\times10^{-2}$ | $-1.02\times10^{-1}$ |

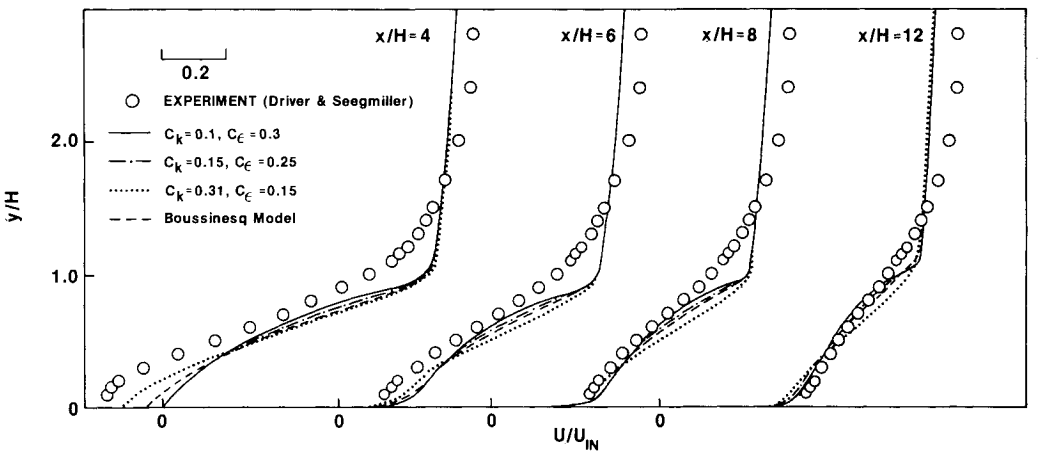


Fig. 3 Mean velocity profiles downstream of the step.

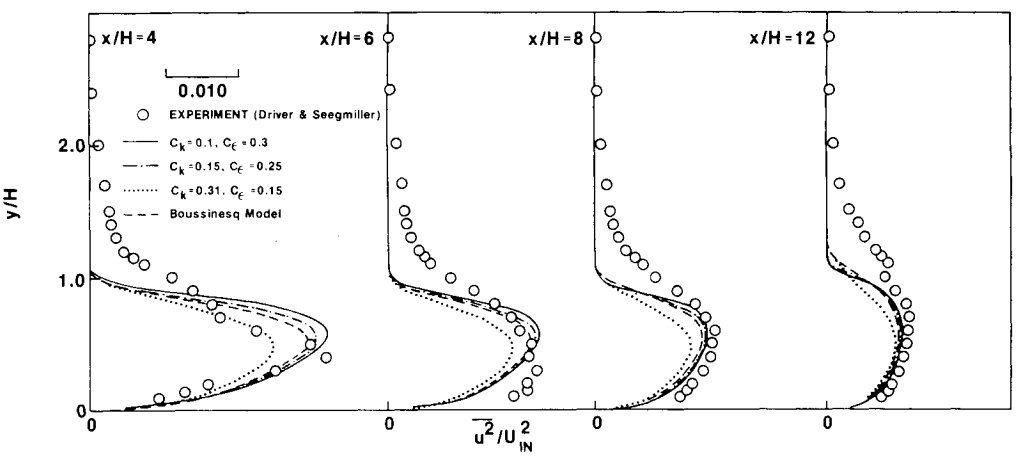


Fig. 4 $\overline{u^2}$ profiles downstream of the step.

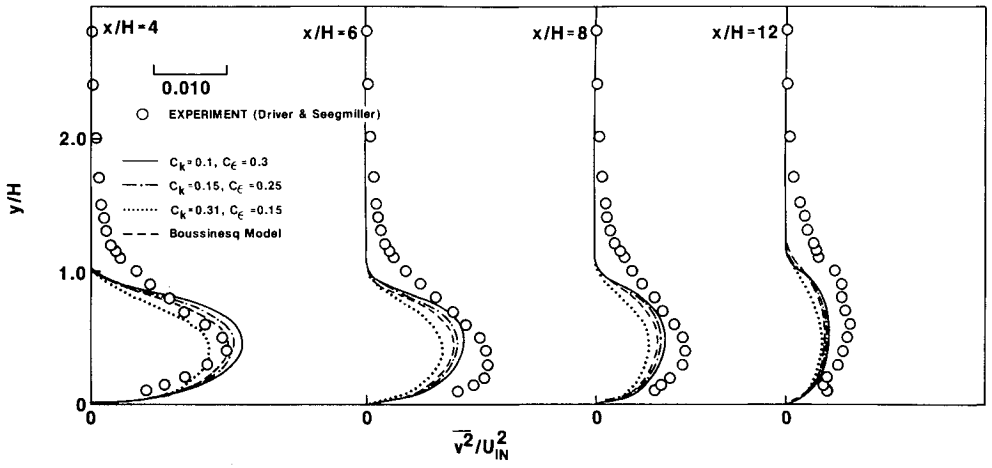


Fig. 5 $\overline{v^2}$ profiles downstream of the step.

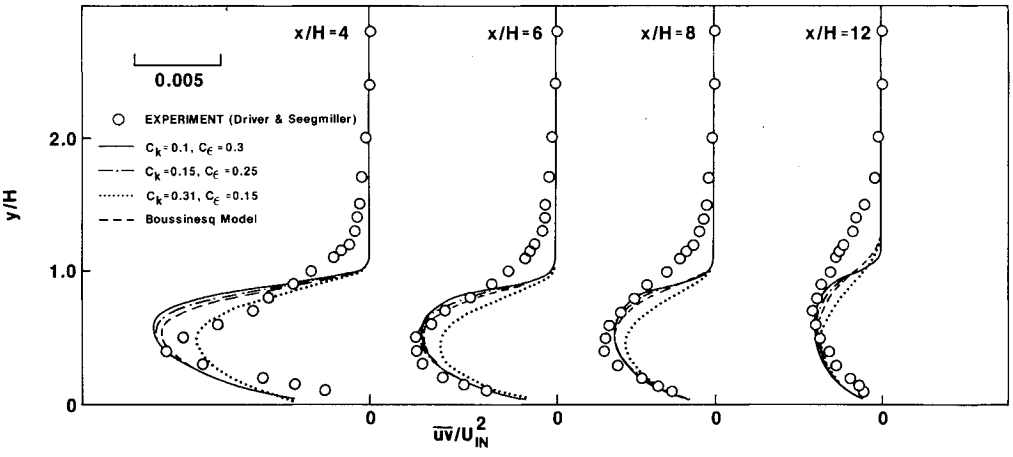


Fig. 6 $\overline{uv}$ profiles downstream of the step.

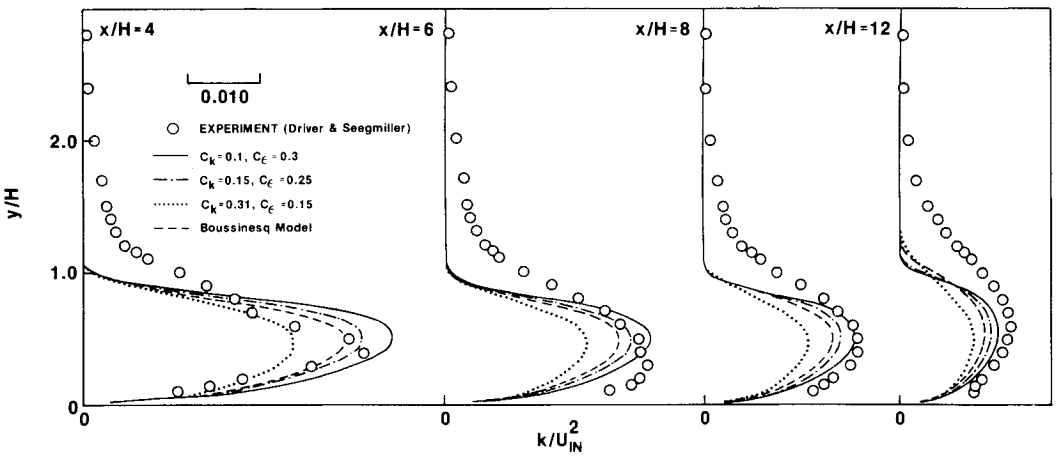


Fig. 7 $k$ profiles downstream of the step.

consists of $60 \times 4$ $H$ with the upper boundary being an inviscid core flow. In both cases, $52 \times 52$ grid points are used with expansion rates of 2 and 3% in the $x$ and $y$ directions, respectively. With these systems, the dimensionless distance to the first grid point from the wall, $y^+$, varies from 7 to 30 along the wall, which is considered to be fine enough to numerically discretize the boundary-layer region of the flow.

## Results and Discussion

Figures 3–7 show the computed results of mean velocity and the Reynolds stresses at several streamwise locations behind the step for $Re_H = 32{,}000$. The typical CPU time consumed for one computation was approximately 30 min on a UNIVAC 1100 with about 300 iterations. It was also found that the CPU time depends slightly on the values of the

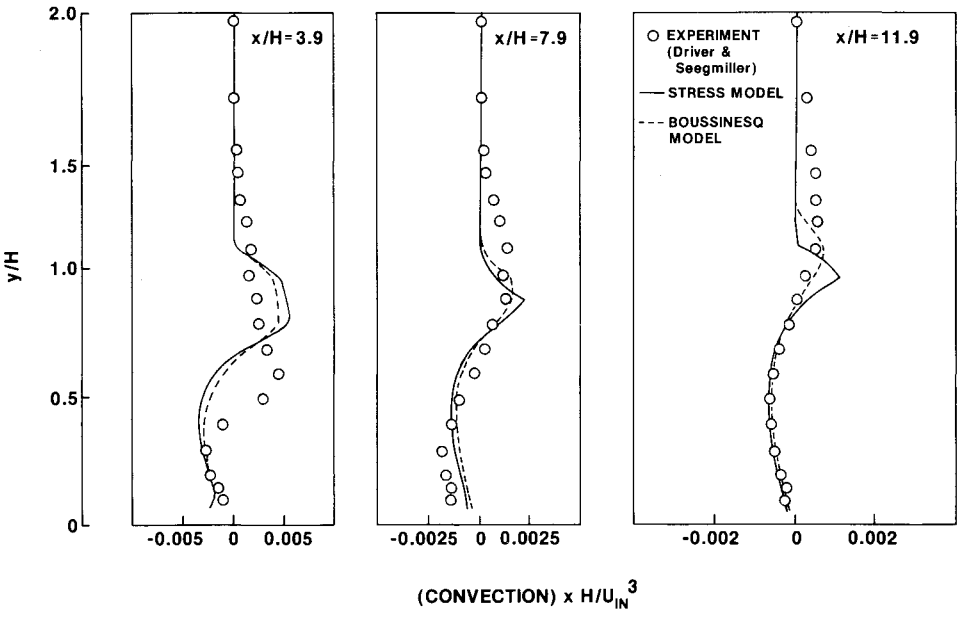


Fig. 8 Convection of turbulence energy.

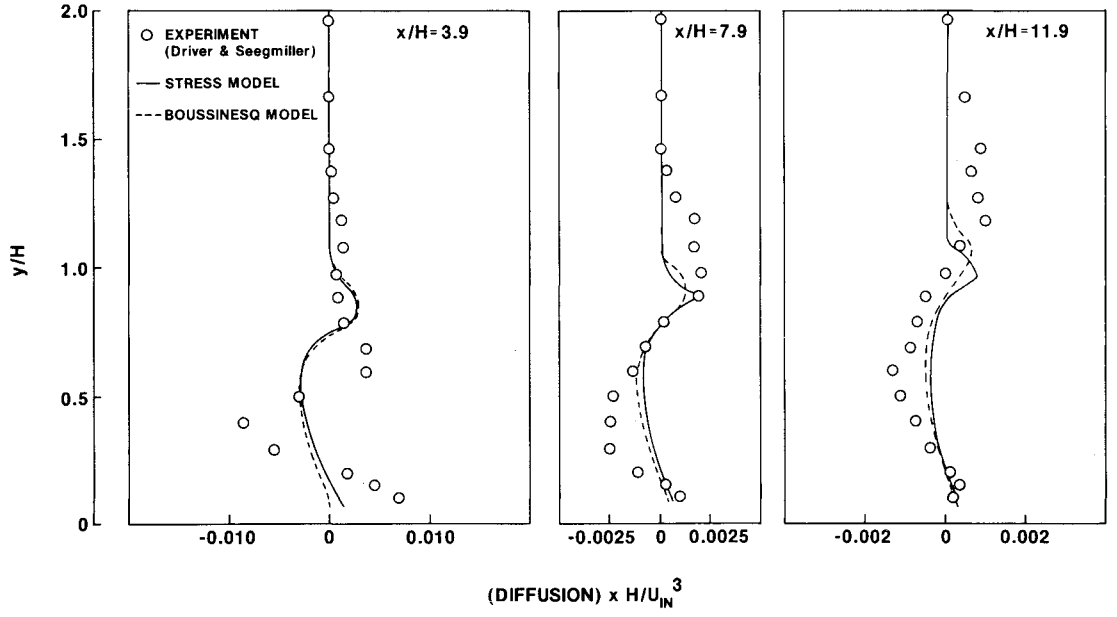


Fig. 9 Diffusion of turbulence energy.

coefficients $C_k$ and $C_\epsilon$ in Eqs. (4) and (8). Namely, the computation with $C_k = 0.31$ and $C_\epsilon = 0.15$ took about 16% more CPU time and 50 additional iterations than the case of $C_k = 0.1$ and $C_\epsilon = 0.3$. As shown in these figures, the profiles of the Reynolds stresses computed with the coefficients $C_k = 0.31$ and $C_\epsilon = 0.15$, which are recommended to date for free-mixing layers or wakes, are much lower than shown in the experimental data of Driver and Seegmiller[6]: about 20–30% lower for the normal stresses and 14% lower for the shear stresses.

In order to improve the prediction of these turbulence stresses in the reattaching shear layer, a number of parametric tests have been performed for different values of the diffusion coefficients. It was discerned that the smaller values for $C_k$ and the higher values for $C_\epsilon$ give better results in comparison with measured data. This is because the large $C_k$ tends to increase the diffusion of turbulence energy, resulting in lower levels of the Reynolds stresses. Similarly, the smaller $C_\epsilon$, in turn, increases the dissipation rate of the turbulence energy, which results in a reduction in the turbulence energy. It should be noted that the recirculating flow at the corner of the step and the bottom wall enhances the level of turbulence energy in the separated flow, resulting in much higher energy at the reattaching region, and this energy is transported downstream.

After performing parametric tests, it was found that the combination of $C_k = 0.1$ and $C_\epsilon = 0.3$ gives the optimum results for both the mean velocity and the Reynolds stresses. It is also observed in Figs. 3–7 that even the Boussinesq model§ gives better results than the Reynolds-stress model with the originally recommended diffusion coefficients. The

§The Boussinesq model has the diffusion term in the following form: $D_\phi = (\partial/\partial x_\ell)[0.09(k^2/\sigma\epsilon)(\partial\phi/\partial x_\ell)]$ where $\phi$ represents $k$ or $\epsilon$ and $\sigma$ stands for the Prandtl number for $k$ or $\epsilon$.

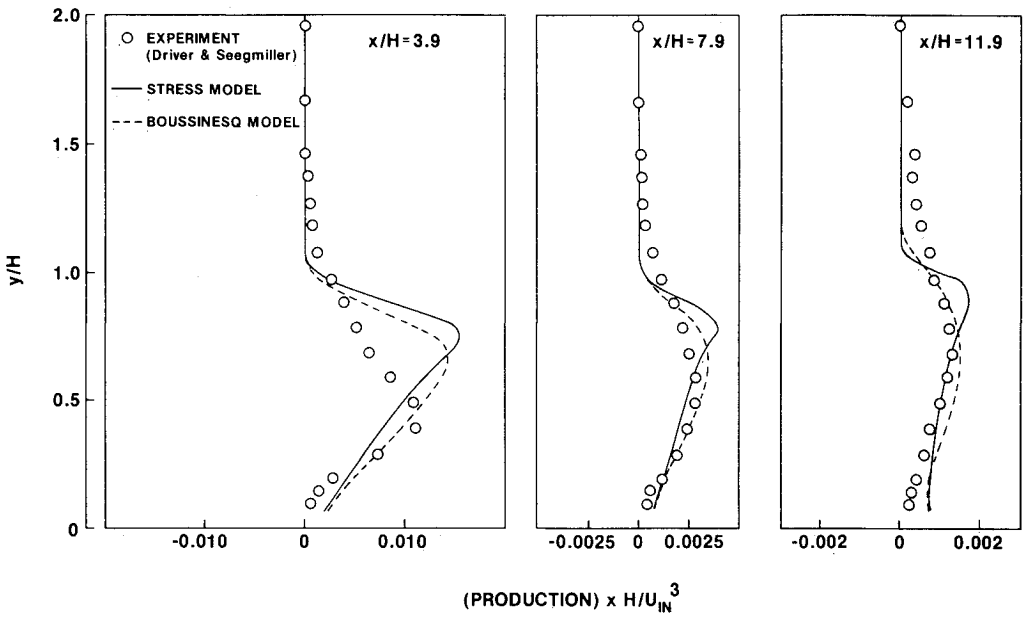


Fig. 10 Production of turbulence energy.

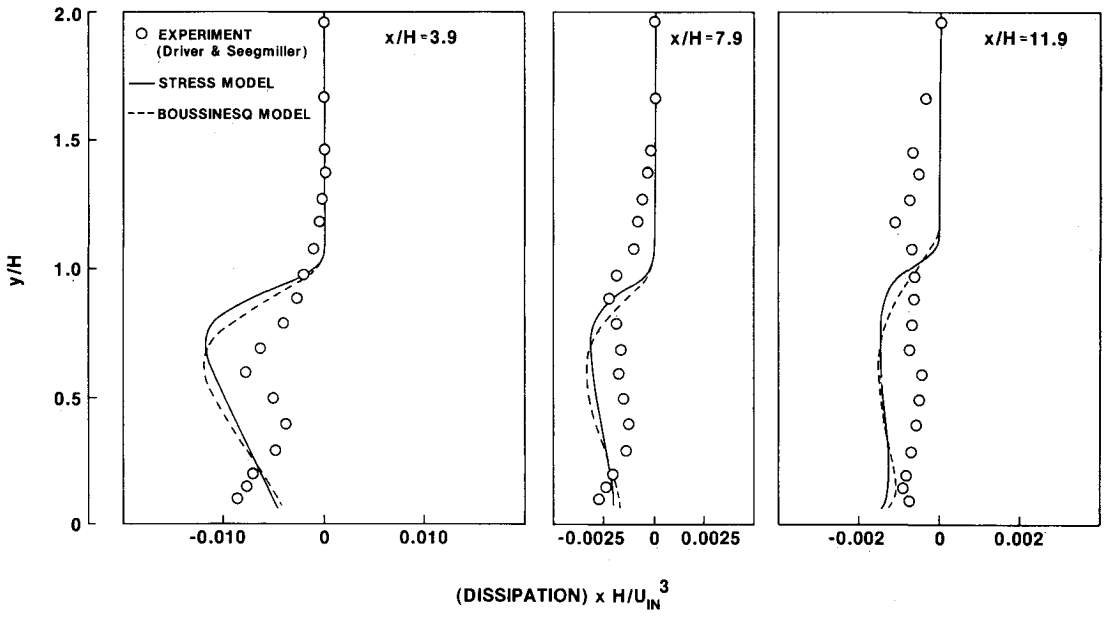


Fig. 11 Dissipation of turbulence energy.

improvement made by the Reynolds-stress model with the new coefficients $C_k = 0.1$ and $C_\epsilon = 0.3$ is primarily attributed to the inclusion of the Reynolds stresses, which account for the nonisotropic effects.

The turbulence energy balance is examined by using both the present Reynolds-stress model and the Boussinesq model and is given in Figs. 8–12. The distributions of the convection term (Fig. 8) show that both models give equally reasonable levels at several different locations. For the distributions of the diffusion term, however, the computed results do not agree well with the experimental data in the recirculating region, as exemplified at $x/H = 3.9$ in Fig. 9. This is the reason why the triple-velocity products are examined by using the transport equations for $\overline{u_i u_j u_k}$, as shown in the next subsection. Both the computed distributions of the production rate (Fig. 10) and the dissipation rate (Fig. 11) are relatively in accordance with the experimental data, although both models always slightly overpredict these quantities.

The overall balance of these terms is compared with the experimental data in Fig. 12. Here the computations are made by using the Reynolds-stress model with the presently recommended diffusion coefficients. It is observed that both the production and dissipation rates predominate in the shear layer near the step, but these levels decay quickly downstream of the step. In contrast, the diffusion and convection rates remain almost constant in the streamwise direction, while they vary rapidly in the transverse direction.

The computed distribution of wall static pressure along the wall is shown in Fig. 13. The results are also compared with the data obtained by Driver and Seegmiller.[6] The agreement is generally reasonable except that the computations show about a 15% higher level in the fully developed flow region.

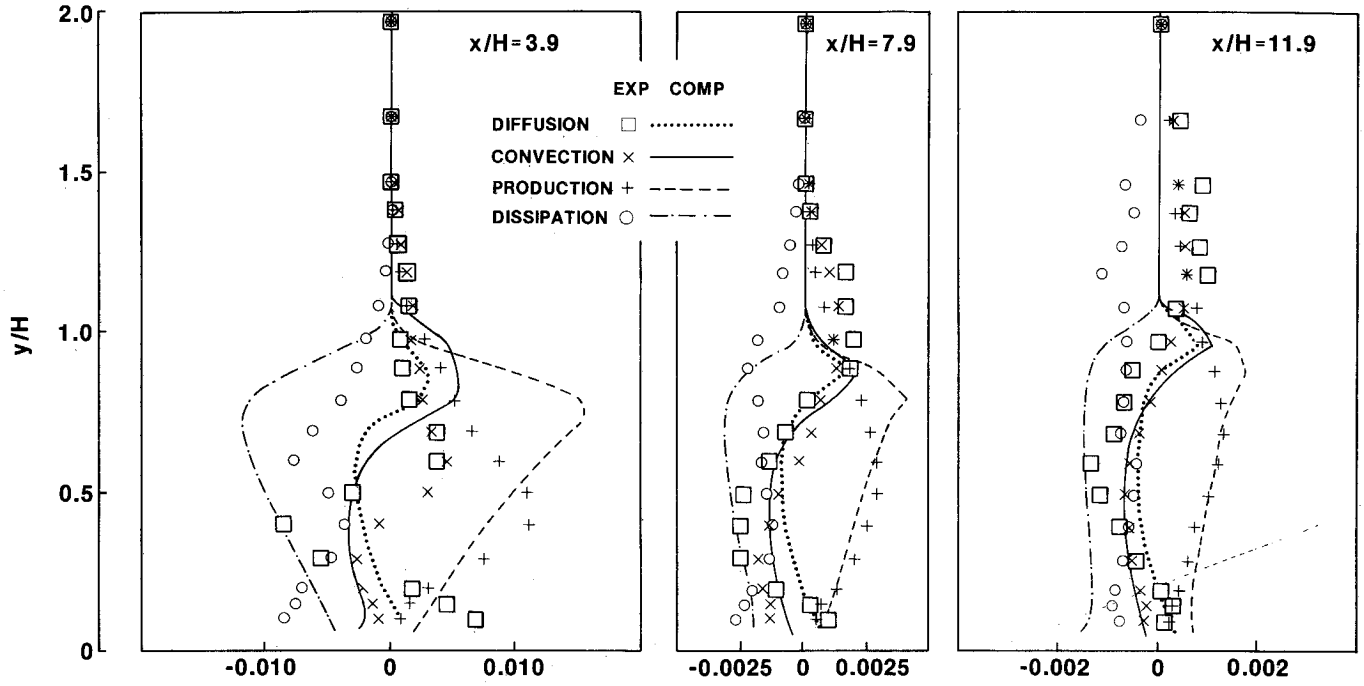


Fig. 12 Turbulence energy balance.

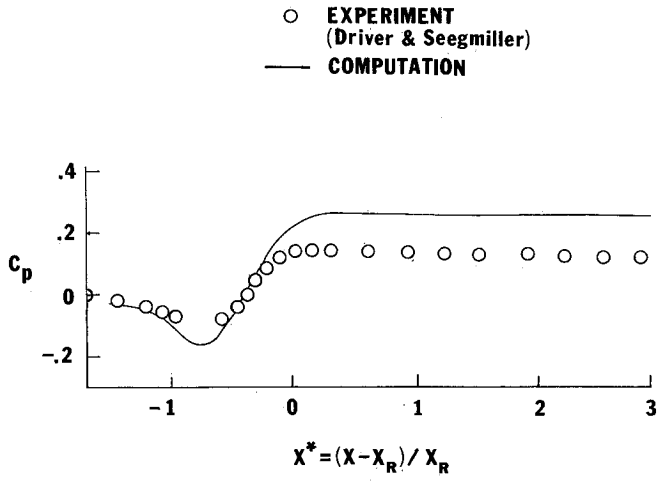


Fig. 13 Wall static pressure distribution.

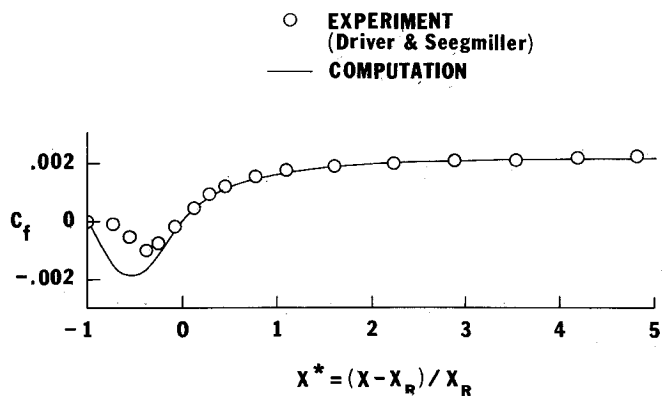


Fig. 14 Skin-friction distribution.

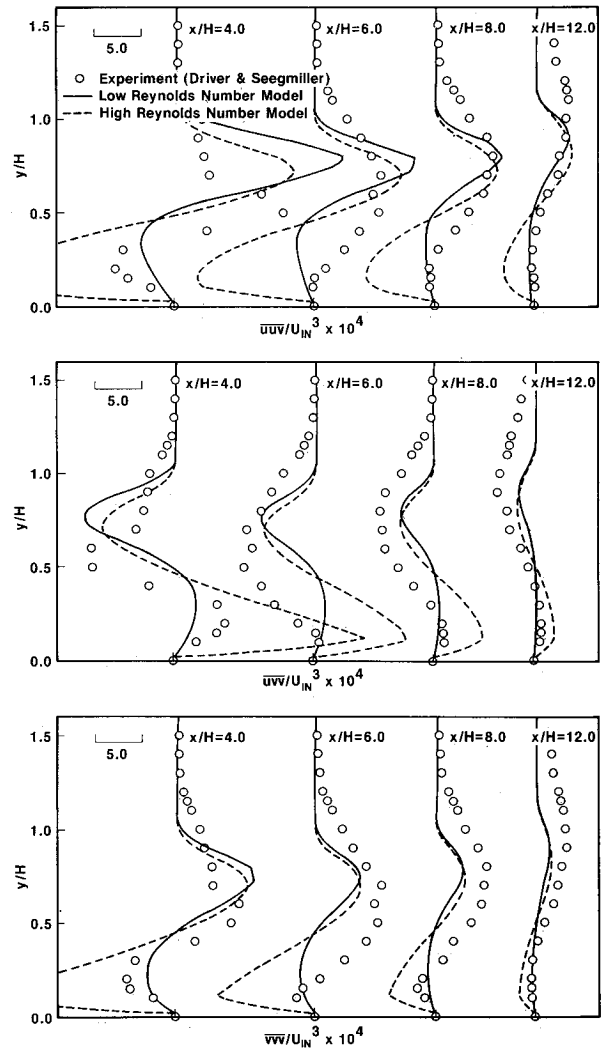


Fig. 15 Triple-velocity products computed by using low- and high-Reynolds-number models.

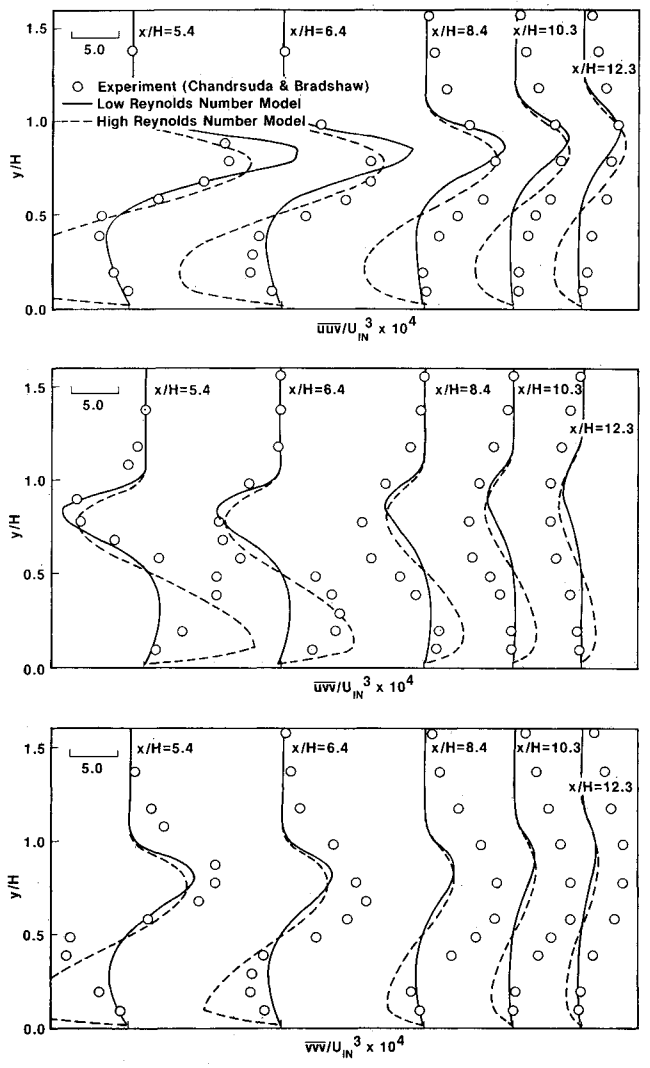


Fig. 16 Triple-velocity products computed by using low- and high-Reynolds-number models.

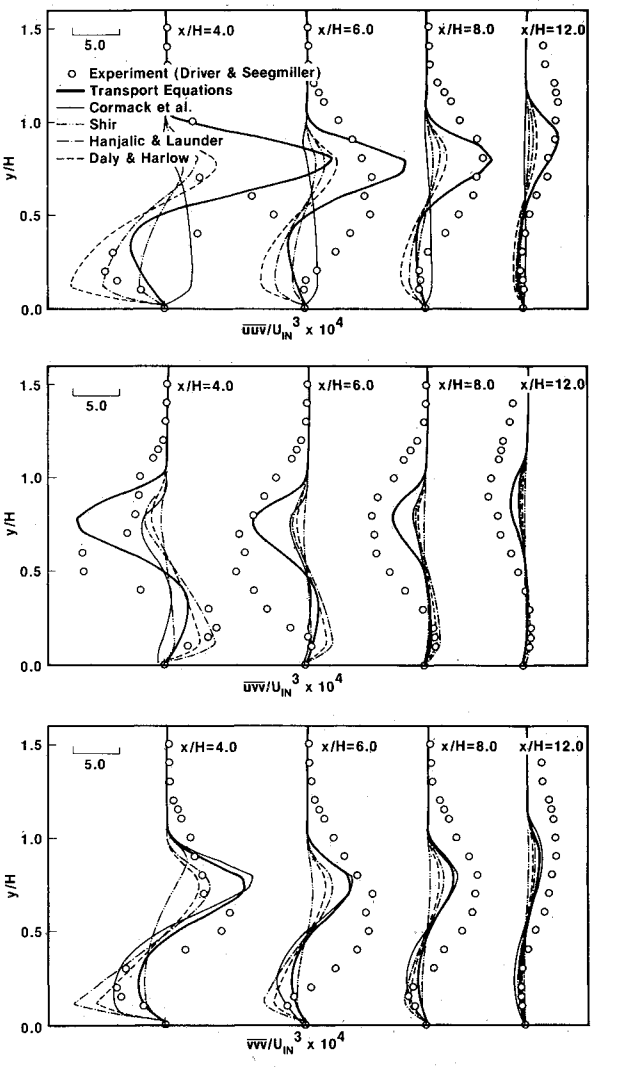


Fig. 17 Triple-velocity products.

The computed distribution of wall shear stress is also compared with the data of the same source and is shown in Fig. 14. The experimental data were obtained by using the oil-flow laser interferometer. The agreement between the computed results and the measurements is much better than that of the pressure coefficient.

In order to establish a reliable model for the prediction of the third-moments in the reattaching shear layer, the values of the mean velocities and the second-moments are initially solved to enable the solution of the transport equations for $\overline{u_i u_j u_k}$. In this way, the existing models for the triple-velocity products are also evaluated and compared with the present third-moment closure model. The values of the mean velocities, $\overline{u_i u_j}$, $k$, and $\epsilon$, computed with the method described in the preceding section are stored, and these values are retrieved when the transport equations for $\overline{u_i u_j u_k}$ are computed.

Since Eq. (12) represents the transport equations of $\overline{uuu}$, $\overline{uuv}$, $\overline{uvv}$, and $\overline{vvv}$ in a two-dimensional coordinate system and all four components are coupled among themselves, these four transport equations are solved iteratively. The iteration was terminated when the relative residual source of each equation dropped below $3 \times 10^{-12}$.

Figures 15 and 16 compare the computed triple-velocity product profiles by using the low- and high-Reynolds-number models described previously with the experimental data of Driver and Seegmiller[6] and of Chandrsuda and Bradshaw,[5] respectively. As shown in these figures, the results are improved considerably by using the low-Reynolds-number model, particularly in the near-wall region.

The reason for the improved performance of the presently proposed low-Reynolds number model is that the diffusion transport is appreciably enhanced in the near-wall region by adding the dissipation relation for the boundary-layer flows. Thus, the energy of the triple-velocity correlation is diffused in the near-wall region due to the small-scale eddies.

Figures 17 and 18 show the triple-velocity correlation profiles computed by using the four different algebraic models; these results are also compared to the computations with the low-Reynolds-number model. As shown in these figures, the low-Reynolds-number model gives results much closer to the experimental data than do the other models.

Probably one of the most noteworthy advantages of using the transport equation model for the prediction of the third-moment velocity fluctuations is that this model can take the effects of convection, diffusion, and the generation of $\overline{u_i u_j u_k}$ into account in the computations of complex turbulent flows. Moreover, the transport equations possess a symmetry property in all three directions. Thus, predictions with this model are equally reliable in inhomogeneous flows as well as in homogeneous ones.

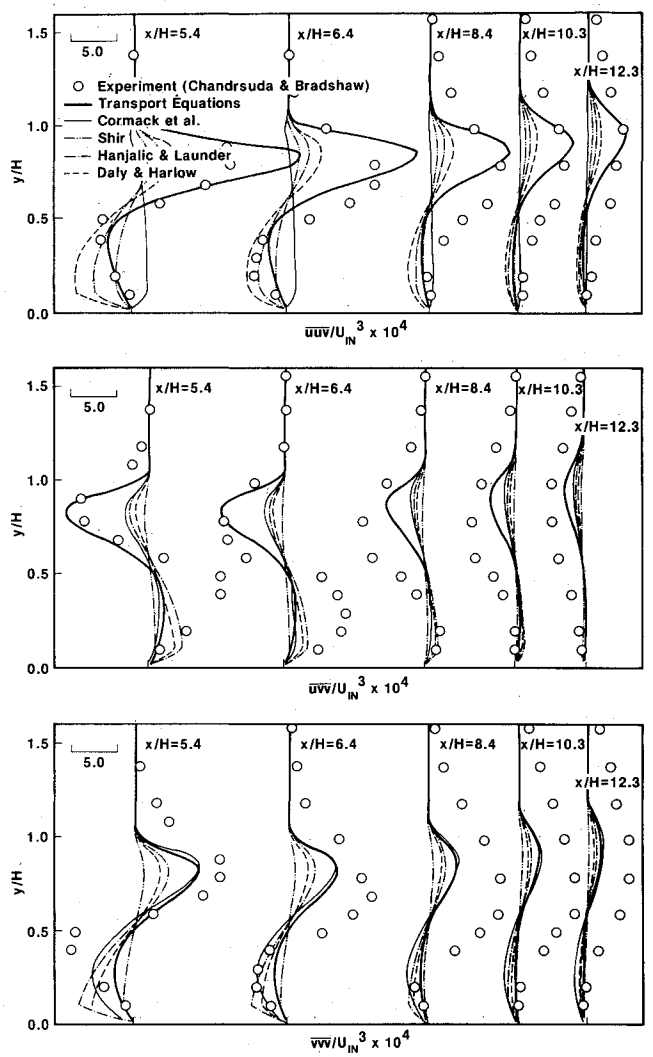


**Fig. 18 Triple-velocity products.**

## Conclusions

1) The diffusion coefficient of the turbulence energy for the computation of reattaching shear layers should be smaller than the commonly used value for free-mixing layers.

2) The diffusion coefficient for the dissipation rate equation was found to be larger for the computation of reattaching layers than for free-mixing layers.

3) The production and dissipation rates of the turbulence energy predominate in the region upstream of the reattachment point, but they decay rapidly downstream from it. In contrast, the convection and diffusion rates do not change appreciably in the streamwise direction.

4) The low-Reynolds-number transport model for the third-moment of the turbulence velocity fluctuations improves the prediction of triple-velocity correlations compared with algebraic models.

## Acknowledgment

This work is supported by NASA Lewis Research Center under Grant NAG 3-546, "A Study of Reynolds Stress Closure Model." The program monitor is Mr. Thomas VanOverbeke.

## References

[1]Eaton, J.K. and Johnston, J.P., "A Review of Research on Subsonic Turbulent Flow Reattachment," *AIAA Journal*, Vol. 19, Sept. 1981, pp. 1093–1100.

[2]Etheridge, D.W. and Kemp, P.H., "Measurements of Turbulent Flow Downstream of a Rearward-Facing Step," *Journal of Fluid Mechanics*, Vol. 86, 1978, pp. 545–566.

[3]Kim, J., Kline, S.J., and Johnston, J.P., "Investigation of a Reattaching Turbulent Shear Layer: Flow Over a Backward-Facing Step," *Journal of Fluids Engineering*, Vol. 102, 1980, pp. 302–308.

[4]Smyth, R., "Turbulent Flow Over a Plane Symmetric Sudden Expansion," *Journal of Fluids Engineering*, Vol. 101, 199, pp. 348–353.

[5]Chandrsuda, C. and Bradshaw, P., "Turbulence Structure of a Reattaching Mixing Layer," *Journal of Fluid Mechanics*, Vol. 110, 1980, pp. 171–194.

[6]Driver, D.M. and Seegmiller, H.L., "Features of a Reattaching Turbulent Shear Layer in Divergent Channel Flow," *AIAA Journal*, Vol. 23, Feb. 1985, pp. 163–171.

[7]Daly, B.J. and Harlow, F.H., "Transport Equations in Turbulence," *The Physics of Fluids*, Vol. 13, No. 11, 1970, pp. 2634–2649.

[8]Shir, C.C., "A Preliminary Numerical Study of Atmospheric Turbulent Flows in the Idealized Planetary Boundary Layer," *Journal of Atmospheric Science*, Vol. 30, 1973, pp. 1327–1339.

[9]Hanjalic, K. and Launder, B.E., "A Reynolds Stress Model of Turbulence and Its Application to Thin Shear Flows," *Journal of Fluid Mechanics*, Vol. 52, Part 4, 1972, pp. 609–638.

[10]Cormack, D.E., Leal, L.G., and Seinfeld, J.H., "An Evaluation of Mean Reynolds Stress Turbulence Models: The Triple-Velocity Correlation," *ASME Journal of Fluids Engineering*, Vol. 100, 1978, pp. 47–54.

[11]Amano, R.S. and Goel, P., "Triple-Velocity Products in a Channel with a Backward-Facing Step," *AIAA Journal*, Vol. 24, June 1986, pp. 1040–1043.

[12]Rotta, J.C., "Statistische Theorie Nichthomogener Turbulenz," *Zeitschrift fur Physik*, Vol. 129, 1951, pp. 547–572.

[13]Launder, B.E., Reece, G.J., and Rodi, W., "Progress in the Development of a Reynolds-Stress Turbulence Closure," *Journal of Fluid Mechanics*, Vol. 68, 1975, pp. 537–566.

[14]Pope, S.B. and Whitelaw, J.H., "The Calculation of Near-Wake Flows," *Journal of Fluid Mechanics*, Vol. 73, 1976, pp. 9–32.

[15]Amano, R.S. and Goel, P., "Improvement of the Second- and Third-Moment Modeling of Turbulence," NASA CR-176478, 1986.

[16]Patankar, S.V., *Numerical Heat Transfer and Fluid Flow*, McGraw-Hill, New York, 1980.

[17]Amano, R.S., "Development of a Turbulence Near-Wall Model and Its Application to Separated and Reattached Flows," *Numerical Heat Transfer*, Vol. 7, No. 1, 1984, pp. 59–75.

[18]Amano, R.S. and Goel, P., "Computations of Turbulent Flow Beyond Backward-Facing Steps by Using Reynolds-Stress Closure," *AIAA Journal*, Vol. 23, Sept. 1985, pp. 1356–1361.